

# An XYZ Gap-Closing Microstage Actuator Based on a Two Mask SOI Process

Nikolaos Chronis and Kwok-Siong Teh

Department of Mechanical Engineering

University of California, Berkeley, CA 94720-1740

Email: ksteh@newton.berkeley.edu

## ABSTRACT

In this work, the design, fabrication process and theoretical characterization of an XYZ gap-closing microstage actuator based on a simple, two-mask silicon-on-insulator (SOI) process is presented. An aluminum thin film is selectively deposited on the serpentine supporting springs of the actuator forming a bimorph structure. The lattice mismatch between silicon and the aluminum film introduces a tensile stress on the metal film, which upon the structure being released, contracts and causes the bimorph supporting spring to bend out of plane, enabling the Z downward motion of the stage. By applying adequate potential differences between the substrate and the structure, as well as between the gap-closing drive actuators and the structure, the structure can be manipulated in a three-dimensional fashion.

**Keywords:** SOI process, gap-closing actuator, bimorph

## INTRODUCTION

As more MEMS structures enter the realm of commercialization, ease and cost of fabrication, device performance versatility and structural reliability have become some of the most challenging issues to contend with. In the recent years, optical and RF MEMS has become one of the fastest growing research and development area of MEMS. Some of the more prominent applications include optical/RF microswitches, micromirror arrays and micro-confocal lens for biological applications [1,2]. In these applications, out of plane displacement has always been a challenge, due mainly to the current limitations of reliable, available fabrication processes. Previously, vertical electrostatic actuator has been fabricated using deep reactive ion etch (DRIE) followed by trench refill method [3,4]. In another approach, electrostatically actuated closed loop controlled reflector membrane composed of gold coated silicon nitride have also been attempted to fabricate light modulator that can be actuated vertically [5]. The former method is time-consuming due to the need to refill trenches with polysilicon using LPCVD, while the latter method suffers from having many layers that require precise alignment, thus increasing the probability of

misalignment and the cost of fabrication. In yet another approach, Helmbrecht et al [6], exploit the residual stress in a nickel-polysilicon bimorph flexures to raise a single crystal silicon (SCS) micromirror, and then electrostatically manipulate its vertical motion.

In this paper, we propose a combined vertical and lateral moving gap-closing actuator design based on a simple, two-mask SOI process. A layer of a thin aluminum film is sputtered on top, resulting in out of plane bending of the structure upon release. Electrostatic force is then applied to actuate it down and laterally.

## DESIGN AND FABRICATION

Figure 1 shows the schematic of the proposed differentiated-height gap-closing actuator built on an SOI wafer. The vertical motion is induced by the potential difference between the movable structure and the silicon substrate. Lateral motions are induced by the potential difference between each of the four drive actuators and the movable structure.

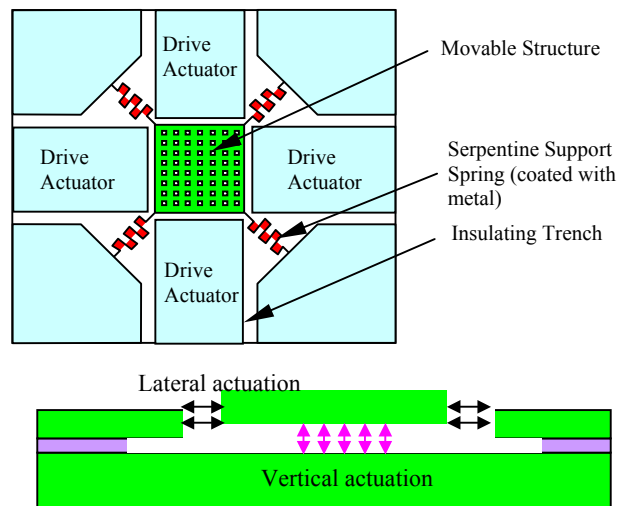


Figure 1. A schematic of the SOI gap-closing actuator and the actuation principle

The SOI fabrication procedure is comprised of a two-mask process (fig.2). The first mask defines the region where Al will be patterned, while the second mask defines the regions where all the mechanical structures

and drive actuators are located. The process begins with an Al deposition by sputtering, which is subsequently followed by a lift-off process in acetone. After the metal is patterned, a second lithographic step is performed to define the region where the movable structure, the serpentine spring as well as the insulating trench are located. Upon hard-baking the photoresist, the pattern is etched by means of a DRIE step that terminates at the silicon-silicon oxide interface. Finally, the structure is released in darkness using 49% concentrated hydrofluoric acid (HF).

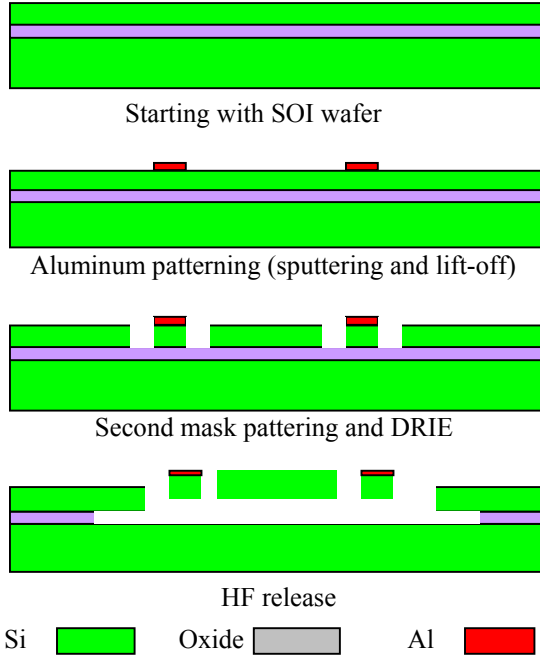


Figure 2: The two masks SOI fabrication process

The absence of photons is crucial in order to ensure that electrochemical etching of Al by HF is minimized, by preventing the formation of a galvanic couple between Al and silicon.

## ANALYTICAL AND NUMERICAL MODELING

We used a combination of analytical expressions and finite element method modeling to predict the performance of the device.

### Spring constants

Although analytical expressions exist for calculating the spring constant of a serpentine spring in three dimensions, those expressions quickly become cumbersome for springs with many meanders. ANSYS<sup>TM</sup> FEM software is used to calculate the

stiffness of a typical serpentine spring having 7 beams, each 200  $\mu\text{m}$  long and 4  $\mu\text{m}$  width, as shown in figure 3.

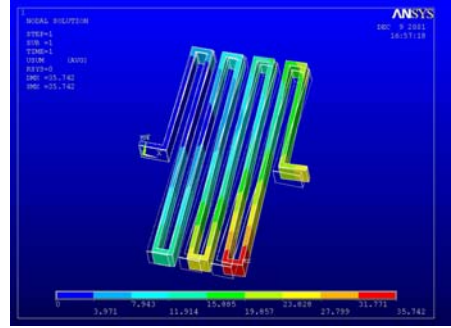


Figure 3: The FEM model of the laterally elongated serpentine spring

The resulting spring constant is 14.3  $\mu\text{N}/\mu\text{m}$  in the z direction and 2.32  $\mu\text{N}/\mu\text{m}$  in the combined x-y direction, since the spring is actually elongated in both directions at the same time.

### Residual stress

The initial displacement of the stage depends on the residual stress of the aluminum film after deposition. The total stress in a thin film typically is the sum of any intentional extended applied stress, the thermal stress and different intrinsic components [7]:

$$\sigma_{tot} = \sigma_{th} + \sigma_{int} + \sigma_{ext} \quad (1)$$

Neglecting any intrinsic and external components, the stress on a thin film is given by:

$$\sigma_{tot} = \sigma_{th} = \left( \frac{E}{1-\nu} \right) \epsilon_{th} \cdot \epsilon_{th} = (a_{Al} - a_{Si})(T_d - T_0) \quad (2)$$

Where the Young's modulus and the Poisson's ratio of the film act independently of orientation, and the thermal strain depends on the mismatch of the coefficient of the thermal expansion of the substrate ( $\alpha_{Si} = 2.5 \cdot 10^{-6}/^\circ\text{C}$ ) and the film ( $\alpha_{Al} = 25 \cdot 10^{-6}/^\circ\text{C}$ ) and the deposition temperature.

The theoretically computed thermal strain of sputtered aluminum at 350 $^\circ\text{C}$  on the SOI wafer measures  $7.3 \cdot 10^{-3}$  at room temperature. The biaxial modulus ( $E/(1-\nu)$ ), with  $E = 74 \text{ GPa}$  and  $\nu = 0.22$ , equals 94.8 GPa and the residual stress is therefore 692 MPa and tensile.

Experimentally, the residual stress can be estimated by measuring the tip deflection of a bimorph cantilever

beam using a white-light interferometer. As shown in Figure 4, the tip deflection is given by [8]:

$$d = \frac{kL^2}{2} = \frac{3L^2}{4t} \frac{(a_{Al} - a_{Si})(T_d - T_0)}{1 + (E_{Si}t_{Si}^2 - E_{Al}t_{Al}^2)^2 / 4E_{Si}t_{Si}E_{Al}t_{Al}t^2}$$

(3)

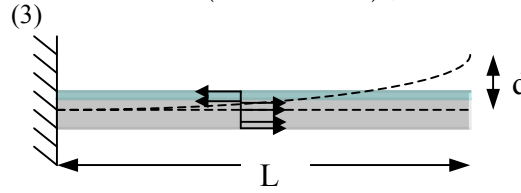


Figure 4: A test structure: The residual stress bends the cantilever upwards. By measuring the tip deflection, the stress can be calculated.

where the term  $(a_{Al} - a_{Si})(T_d - T_0)$  actually represents the thermal strain  $\epsilon_{th}$ . The total film stress can be easily calculated from equation 1, as illustrated in Figure 5.

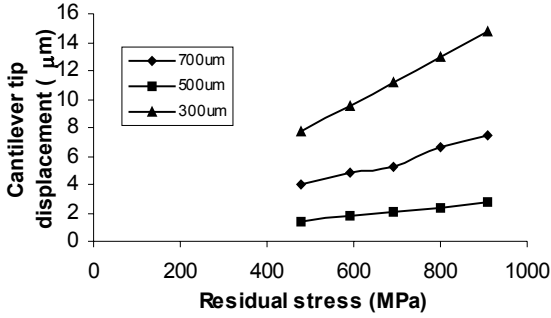


Figure 5: The end displacement of the cantilever test beam of various lengths varies linearly with the residual stress between the Al film and the substrate.

Based on the same idea, the vertical deflection of the spring was modeled using ANSYS. Unfortunately, the expected residual stress is not enough to induce significant amount of vertical displacement. The beam is rather stiff in the Z direction. The FEM model showed elevation of the structure only by 0.4microns. The maximum out of plane of displacement is therefore limited by the buried oxide thickness.

### Electrostatic response

The electrostatic static and dynamic behavior of the actuator was modeled using simple analytical model. First, neglecting fringing field effect, the attractive electrostatic force acting on an element can be approximated by the differential parallel-plate capacitor equation as follows,

$$F_e = \frac{1}{2}\epsilon_0 V^2 A / \delta^2 \quad (4)$$

Where  $\epsilon_0$ , V, A and  $\delta$  represents the permittivity of free space, applied voltage, overlapping area and displacement away from the equilibrium position of the spring. On the other hand, the mechanical force can be expressed as,

$$F_m = k\delta \quad (5)$$

Where  $k$  and  $\delta$  are the mechanical spring, and the displacement away from the equilibrium position, respectively. Hence, by combining equations (1) and (2), the dependence of the applied voltage on the displacement of the movable structure can be expressed as,

$$V = [2k\delta^3 / \epsilon_0 A]^{1/2} \quad (6)$$

Figure 6 shows the required voltage for actuating the movable structure in the X, Y and Z direction for the spring over its equilibrium position in the respective direction. As the area of overlap between the movable structure and the drive actuators is significantly smaller than the overlap area between the movable structure and the substrate, the voltage required to actuate the movable structure in the horizontal direction (X or Y) is significantly larger than the one required for actuation in the Z-direction.

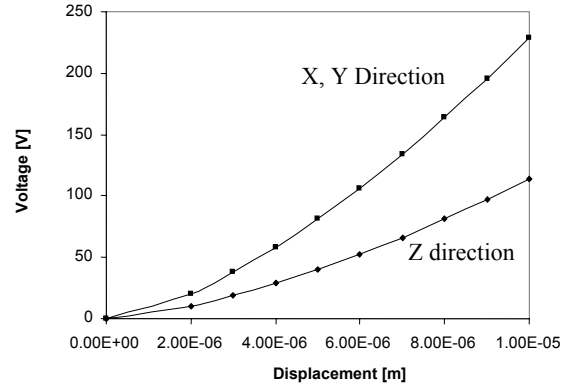


Figure 6: The required voltage for actuating the movable structure in the X, Y and Z direction over the displacement moved in the respective direction.

The resonant frequency of the beam in the Z direction has been analytically calculated to be around 70kHz, and in the X and Y direction to be approximately 28.2kHz. This is reasonable considering the fact that the spring constant in the horizontal direction is about 6 times smaller than the spring constant in the vertical direction, hence the frequency response should be scaled accordingly.

## CONCLUSIONS

A XYZ electrostatic-driven microstage was presented and theoretically characterized. Independent motion of few microns is possible through resonant frequency sweeping due to the different spring constants in each direction. The XYZ stage can be used as a micromirror for three dimensional optical scanning or as a XYZ micromanipulator.

## REFERENCES

- [1] Sunghoon Kwon, Luke P. Lee, "Stacked Two Dimensional Micro-Lens Scanner for MicroConfocal Imaging Array", to be published
- [2] J. -W. Shin, S. -W. Chung, Y. -K. Kim, B. K. Choi, "Design and Fabrication of Micromirror Array Supported by Vertical Springs.", *The 9<sup>th</sup> International Conference on Solid-State Sensors and Actuators*, June 16-19, Chicago, USA, 1997.
- [3] A. Selvakumar, K. Najafi, "High Density Vertical Comb Array Microactuators Fabricated Using A Novel Bulk/Polysilicon Trench Refill Technology", *Technical Digest, Solid-State Sensor and Actuator Workshop*, pp. 138-41, Hilton Head, SC, USA, 1994.
- [4] A. Selvakumar, K. Najafi, W. H. Juan, S. Pang, "Vertical Comb Array Microactuators", *Proc. IEEE Micro Electro Mechanical Systems 1995*, pp. 43-8, Amsterdam, Netherlands, 1995.
- [5] T. Bifano, "MEMS Deformable Mirror for Adaptive Optics", *Solid-State Sensor and Actuator Workshop*, Hilton Head, SC, USA, 1998.
- [6] M. Helmbrecht, U. Srinivasan, C. Rembe, R. T. Howe, R. S. Muller, "Micromirrors for Adaptive-Optics Arrays", *The 11<sup>th</sup> International Conference on Solid-State Sensors and Actuators*, Munich, Germany, June 10-14, 2001.
- [7] Marc Madou, *Fundamentals of Microfabrication*, CRC Press LLC, New York, 1997.
- [8] W. Chu, M. Mehregany, R. Mullen, "Analysis of tip deflection and force of a bimetallic cantilever microactuator", *J.Micromech. Microeng.* 3 (1993)